4.1.2.8 Radio bursts of the non-thermal sun

Arnold O. Benz

The time scale of the radio flux of the sun varies over nine orders of magnitude ranging from milliseconds to months. The shortest are observed during flares in decimetric spikes, the longest origin from the evolution of active regions. The distinctions and classifications by radio astronomers should not be considered as semantic sophistry, but as attempts to understand different physical causes and emission processes. The emission varying slowly with the time scale of active region developments is named S-component and has been described in the previous chapter.

4.1.2.8.1 Solar radio bursts

Enhancements shorter than about one hour form a clearly distinct domain of phenomena. These emissions are superimposed on the quiet solar radiation and often exceed it by many orders of magnitude, particularly at long wavelengths. For this reason they are called "outbursts" or simply "bursts". The burst emission is generally associated with active regions (the space above sunspots in the photosphere and/or chromospheric plages). Nevertheless, comparable radiation has been found e.g. at centimeter wavelength emission of nanoflares in quiet regions, but at four orders of magnitude lower levels.

The burst emission originates in small regions of the solar corona, requiring very high brightness temperatures to yield the observed flux densities. This indicates that some of the emissions are not thermal and do not originate from single particles, but are emitted coherently: Particles that emit the radio emission act together in phase. In the most important such mechanism, waves in the plasma couple with each other to produce radio waves. As many electrons cooperate in phase, such a process is called "coherent" and can reach extremely high brightness temperature. Such waves, including direct excitation of radio waves (called maser), are driven unstable by non-thermal particle distributions. In particular electrons having a non-Maxwellian distribution in velocity are prone to excite waves. The most prominent *incoherent* emission process observed in bursts is weakly relativistic synchrotron radiation, termed gyro-synchrotron emission. There is also thermal burst emission at millimeter waves when the hot flare plasma emits thermal bremsstrahlung radiation. Table 1 summarizes the emission processes proposed for radio burst radiation.

To interpret radio bursts, a physical cause providing the energy and an emission mechanism converting it into radio emission must be identified. The initial energy is generally assumed to be magnetic and is identical to all radio bursts. The release of free magnetic energy manifests itself in flares, but seems to be more general and related to the dynamics of the corona. Radio bursts not associated with flares include noise storms (related to emerging active regions) and moving sources related to coronal mass ejections.

Radio bursts of the active sun are conveniently grouped into decades of wavelength (Table 2). As the sun is not bound to the metric system, the limits of these groups are not taken to be strictly. The grouping according to wavelength has its origin in the emission processes that radiate

Table 1. Emission processes proposed for solar radio bursts of the active sun.

Electron velocity distribution	Coherent emission processes	Incoherent emission processes
thermal	–	bremsstrahlung, gyro-magnetic
non-thermal	plasma emission, electron maser	gyro-synchrotron

Table 2. Regimes of radio bursts of the active sun.

Wavelength regime	Frequency range	Source location	Plasma characteristic	Types
Decameter	20 kHz – 80 MHz	far corona, solar wind	open field lines	I–IV, split pair drift pair
Meter	30 MHz – 600 MHz	upper corona		I–V
Decimeter	200 MHz – 8 GHz	corona	active region flare loop	III, IV, pulsation, spikes
Centimeter	1 GHz – 500 GHz	corona	gyro-synchrotron thermal flare	continuum continuum

at characteristic frequencies, such as the plasma frequency or the electron gyro-frequency. Thus different layers, having different plasma characteristics, radiate in different wavelength regimes.

4.1.2.8.1.1 Burst classes

Decametric bursts

The frequency range of radio sources in the far corona and inner heliosphere corresponds to the metric, decametric, hectometric, and kilometric bands. Only the metric and a small part of the decametric range can be accessed from the ground. The longer wavelengths are blocked by the terrestrial ionosphere and require observations from space.

Noise storms are the most common manifestation of solar activity at meter and decameter waves. At solar maximum and 125 MHz, noise storms are recorded during 13% of the time [81Hac]. The emission consists of a broad continuum and narrow band peaks, called *Type I bursts*. Continuum and bursts come together, but have varying flux ratios. Noise storms are associated with emerging and growing active regions and last from hours to days. Thus, they assume an intermediate position between the phenomena related to the more gradual development of active regions, manifested in the S-component, and the short radio bursts associated with flares. Observational characteristics of noise storms are summarized in Table 3.

At decameter wavelengths, noise storms change in appearance. Most notably, the bursts change in shape and assume the form of rapidly drifting structures in the spectrogram below about 40 MHz. The drift rate corresponds to upward moving electron beams similar, but slightly slower than Type III bursts (see metric bursts). For this reason they are called "storm-type III" bursts. Decametric storm-type IIIs and noise storm continua are correlated [70Boi]. Sometimes the storm-type III bursts appear to grow out of a chain of Type I bursts, starting at about the frequency of the chain and drifting to lower frequency [66Han]. Furthermore, new fine structure appears, such as reversed drift pairs and split pair bursts, that is not observed at meter wavelengths. It is interpreted as low-frequency forms of Type I bursts [73Alv].

Metric bursts

Bursts at meter wavelengths have been classified into five types in the 1950s. A summary of their properties is given in Table 4. The emission processes are still uncertain with the exception of Type III bursts. It is assumed to be plasma emission in all burst types at the fundamental or harmonic of the source plasma frequency. With the exception of Type I bursts, all types are related to flares. The observed brightness temperature of all metric bursts can reach the order of 10^{12} K. The observed values are lower limits due to the enlarged size by scattering in the corona. Thus the emission is generally assumed to be non-thermal. More details can be found in the general references [a, b, c, d].

Table 3. Properties of noise storms and Type I bursts [77Elg, 81Ben].

Association	Noise storms are connected to active regions. Nevertheless, the emission region is not exactly above the sunspot group, sometimes rather in between groups.
Position	The position of the bursts scatters around that of the continuum.
Polarization	Continuum and bursts are strongly polarized in the same circular sense. Near the limb, they become depolarized.
Directivity	The emission is directive in radial direction. The mean full width half-power emission angle is of the order of 80°. Individual bursts have widths of only 25°.
Source height	At meter waves, the source regions are at altitudes between 0.1 and 1.0 solar radii above the photosphere.
Size	The size of the emission region is an arcminute for bursts and several arcminutes for the continuum. It increases with wavelength. The minimum size is limited by scattering in the corona (Table 5).
Intensity	The brightness temperature of the continuum is 10^7–10^{10}K, in bursts it can exceed $2 \cdot 10^{11}$ K.
Bandwidth	The bandwidth of bursts is typically 2% of the observed frequency and increases with wavelength.
Duration	The duration of bursts is between 0.1 s and a few seconds. It increases with wavelength.
Fine structure	Often Type I bursts appear in "drifting chains" drifting usually, but not always, to lower frequency. In standard model atmospheres, the drift rate corresponds to an average upward motion of 160 km/s.
Interpretation	The general interpretation assumes emission at the fundamental of the local plasma frequency for both continuum and bursts. Harmonic emission has not been reported.

Table 4. Metric radio bursts of the non-thermal sun. Typical bandwidth and duration are given for a mean frequency of 200 MHz. The typical polarization is given for the center of the disk (low: 0–20%, intermediate: 20–90%, high: 90–100%).

Burst type	Bandwidth [MHz]	Duration [s]	Circular polarization	Suggested energy source	Suggested emission process
I	4	1	high	coronal dynamics	plasma wave turbulence
II	4	300	low	shock wave	shock turbulence and
	20	2	low	electron beam	bump-on-tail instability
III	100	2	intermediate	electron beam	bump-on-tail instability
IV	200	1000	high		loss-cone instability (?)
V	30	20	intermediate	beam instability	(?)

Type II bursts have a characteristic drift of a few MHz/s in frequency at 200 MHz, corresponding to an upward motion of 300–1000 km/s. They consist of two components: a "herring bone" structure of type III-like bursts drifting away from the narrowband "back bone". The former emission is generally interpreted as the signature of electron beams accelerated at a shock front. These beams move both upward and downward in the corona and appear in a spectrogram like the bones of a herring fish. The back bone has been proposed to be the result of plasma wave turbulence at the shock front coupling into radio emission. Back bones are part of every Type II burst, herring bones are less frequent (20%) and are observed only in the lower metric waveband. Type II bursts often show harmonic emission at twice the fundamental structure. The two bands then slowly drift parallel to each other to lower frequencies (Fig. 1).

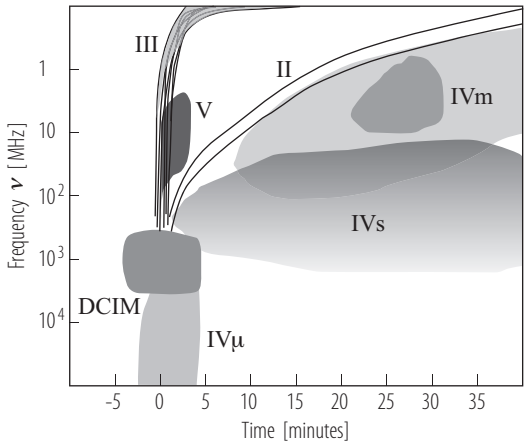

Fig. 1. Schematic overview on flare radio burst emissions. The frequency increases downward on the y-axis to mimic decreasing altitude in the solar corona. Burst types are marked with roman numerals as introduced for metric bursts. Types IVm and IVs distinguish between moving and stationary Type IV bursts, respectively. DCIM (customary for decimetric emissions) includes several burst types defined in Fig. 2. Type IVμ indicates centimeter continuum due to gyro-synchrotron emission. It may continue beyond 100 GHz.

An electron beam moving along magnetic field lines may emit a *Type III* radio burst. It is the best understood radio emission process as it can be observed at the longest wavelengths in interplanetary space in situ. The beam electrons excite plasma oscillations in the plasma they transverse by the bump-on-tail instability. The electrostatic plasma waves couple into radio waves by wave-wave interactions with ion-sound waves (yielding emission at about the plasma frequency) and with an anti-parallel plasma wave (yielding emission at twice the plasma frequency). Since the plasma frequency,

$$\omega_p = \left(\frac{4\pi e^2 n_e}{m_e}\right)^{1/2} \quad , \tag{1}$$

(cgs units) depends only on the electron density n_e, the emission of an upward-going beam has a decreasing frequency. This fast drift in frequency is a characteristic of Type III emission. Type III bursts have been reported over the frequency range from 8.5 GHz to 10 kHz. In the centimeter range, the drift is predominantly positive (downward in the corona). At the low-frequency end, the emission exclusively drifts to lower frequency. There are also Type III bursts following loops and forming U-shaped features in meter wave spectrograms.

Type III radio bursts are the most frequent flare-related emission. In times of solar maximum, there are about 5000 meterwave Type III groups per year. Type III bursts are also the most

frequent burst types in the decimeter and decameter ranges.

The average drift rate at the observing frequency ν in the metric and kilometric band is

$$\frac{d\nu}{dt} = -0.01\nu^{1.84} \quad [\text{MHz s}^{-1}], \tag{2}$$

where ν is in MHz. At decimeter and centimeter wavelengths, the drift rate is approximately

$$\frac{d\nu}{dt} \approx \nu \quad [\text{MHz s}^{-1}], \tag{3}$$

where ν is in MHz. The decay is generally exponential and averages to

$$\tau_d = 5.13 \cdot 10^7 \nu^{-0.95} \quad [\text{s}], \tag{4}$$

over the full range of observed Type III frequencies [73Alv, 92Ben]. The rise time is usually shorter than the decay time.

Radio continua associated with flares are classified as *Type IV* bursts. The class is bewildering as it probably includes various geometries and different physical phenomena. The individuality perceived in spectrograms has led to a confusing number of subtypes. Two types may be distinguished from the point of view of source motion:

- Stationary Type IV bursts appear near the flare site during the impulsive flare phase at the decimeter wavelength and in the post-flare phase at meter wavelength. They may be related to the reordering of the magnetic field due to reconnection in the flare and post-flare phases. In the range 200–1000 MHz, stationary Type IV bursts usually consist of irregular pulsations having well-defined upper and lower bounds in frequency. Stationary Type IV events at meter wavelength may gradually turn into a noise storm.

- Moving Type IV bursts at meter and longer wavelengths appear to be associated with shocks and/or coronal mass ejections. They occur after the impulsive phase emissions of flares and drift in the spectrum to lower frequency. The spectral classification by their drift is not unique, however.

Starting at 1 GHz and peaking between 3 and 20 GHz, the continuum emission is smooth in the spectrum and varies slowly in time with a time constant exceeding one second. The high-frequency slope is a power-law that can be followed into the millimeter range. The emission is generally attributed to gyro-synchrotron radiation. The term "microwave Type IV" burst or "IVμ" is rarely used .

Finally, *Type V* radio bursts form a class introduced to describe the continua observed in the meter wavelength range after intense Type III bursts. The duration is between 10 and 30 seconds at 200 MHz and increases with wavelength. As it seems to be related to electron beams traversing the upper corona, it has been interpreted as the result of a beam instability, leaving behind some electrons in stationary sources.

Decimetric bursts

In the decimeter range, new classes of radio bursts appear. Catalogues with prototypes can be found in the literature [90Gue, 94Isl]. The characteristic bandwidth and duration of individual fine structures defines the five types of decimetric bursts (Fig. 2). Long-duration events, lasting well beyond the impulsive phase of flares, have been already mentioned above under *decimetric Type IV* bursts. They appear in spectrograms in a large variety of forms even in the same flare. Decimetric type IV bursts can last from tens of seconds to several hours. The emission is usually modulated in time on scales of 10 s or less. The strong circular polarization excludes the gyro-synchrotron emission process. Occasionally there are groups of narrowband spikes, apparently forming a part of

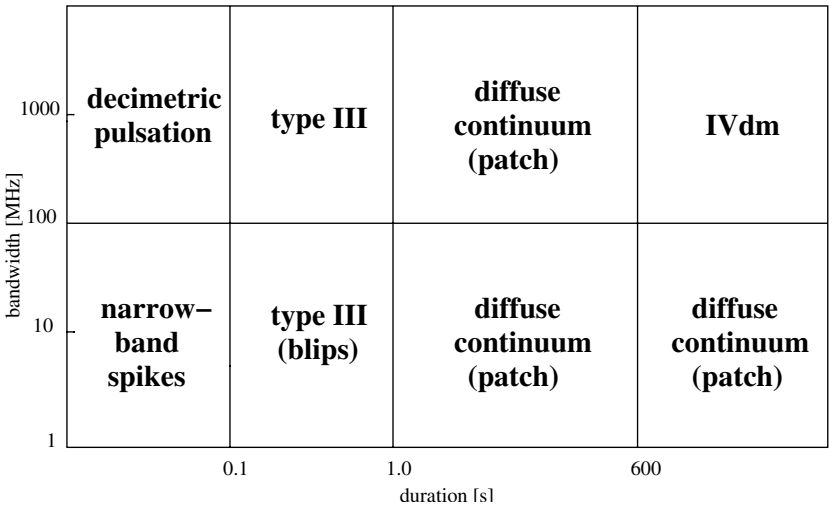

Fig. 2. Schematic overview on the main classes of flare radio bursts at decimeter wavelengths in duration and bandwidth of structural elements [94Isl].

the Type IV burst. Spectral fine structures such as intermediate drift bursts (also called "fibers") and parallel drifting band ("zebra pattern") appear in the whole decimeter range.

Broadband continua forming quasi-regular pulses of more than 100 MHz bandwidth are called *decimetric pulsations*. The pulses are separated by 0.1 to 1 seconds and have similar starting and ending frequencies, contrary to Type III bursts. Furthermore, they are highly polarized, again in contrast to decimetric Type III bursts. Pulsations are well associated and sometimes even correlated with the hard X-ray emission of flares.

Narrowband spikes are also well associated and sometimes correlate with hard X-rays, but are less frequent than pulsations. They form groups consisting of thousands of individual spikes. At 1 GHz, the e-folding decay time of spikes is 13 times shorter on the average than for Type III bursts in same range [90Gue].

Diffuse continua having a bandwidth of typically 10% of the center frequency and 1–10 second duration are most frequent in the 1–3 GHz range. They have also been called "patches", and some have been reported to slowly drift to higher frequency.

Centimetric bursts

Featureless radio bursts above 1 GHz extending up to the submillimeter range are also called "microwave bursts" or Type IVμ. The spectral peak is typically around 10 GHz, but may be between 3 GHz and more than 100 GHz. It is generally interpreted by gyrosynchrotron emission of mildly relativistic flare electrons. Below the spectral peak, the emission is optically thick. Above, it is optically thin, and its spectrum is directly related to energy distribution of the electrons. Gyro-synchrotron emission correlates well in time with the hard X-ray flux, best below 80 keV. At millimeter wavelength, the best correlating X-rays have energies above 500 keV. Gyrosynchrotron emission is weakly polarized. A review on the source properties at different wavelengths is given in [98Bas].

Correlation over three orders of magnitude has been reported between the peak flare fluxes of centimeter flux density and hard X-ray emission > 30 keV (Fig. 3). The relation is linear

$$F_R = 0.08\ F_{HX} \quad [\text{sfu} = 10^{-22}\text{Ws}^{-1}\text{Hz}^{-1}], \tag{5}$$

where F_{HX} is given in hard X-ray counts per second observed > 30 keV by the HXRBS detector equipped with a sensitive area of 71 cm^2. The correlation is generally interpreted as evidence that both emissions originate from the same population of electrons.

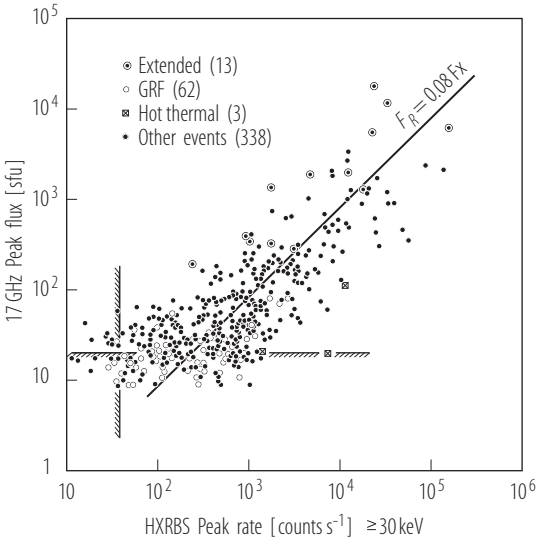

Fig. 3. Peak flux density of flare centimeter (gyrosynchrotron) emission versus hard X-ray peak count rate. The data are collected from 416 flares observed at 17 GHz by the Nobeyama polarimeter and the HXRBS spectrometer on the Solar Maximum Mission. A large majority of flares are impulsive (*black dots*), other flare types are indicated by symbols. The effective sensitivity threshold of the two instruments are indicated by the *shaded lines* [88Kos].

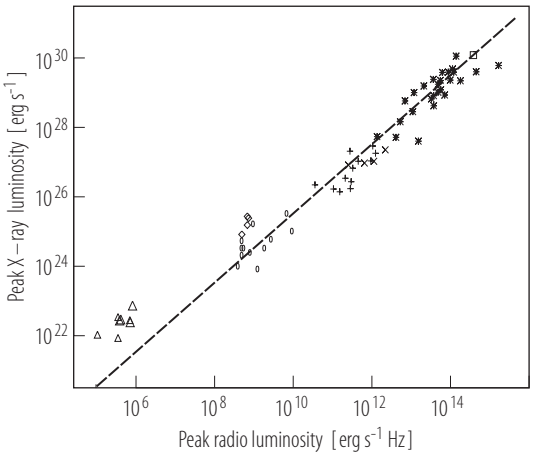

Fig. 4. Peak flux of flare soft X-ray emission versus peak radio luminosity at 3.6 cm. Nanoflares in the quiet sun are presented with the symbol △, microflares in active region by ⋄ and 0, impulsive and gradual solar flares by + and ×, respectively, quiescent dMe, dKe and By Dra stars by ∗, and a long duration flare on the dMe star EQ Peg by ⊓. The dashed line is a fitting curve with slope 1 to the dMe stars given by Eq.(6) [00Kru].

In addition to hard X-rays, the peak centimeter flux density also correlates with the soft X-ray peak flux. The latter is thermal bremsstrahlung emission of the hot flare plasma and is indicative for the total flare energy. The correlation follows a linear relation,

$$F_R = 3.16 \cdot 10^{-16}\ F_{SX} \quad [\mathrm{W\ Hz^{-1}}], \tag{6}$$

where F_{SX} is in units of Watts. Figure 4 shows the relation in graphical form. It extends over more than 8 orders of magnitude and includes also the quiescent emission of active stars consisting of superimposed flares. Only events with decreasing spectrum indicating gyrosynchrotron emission have been selected. Nanoflares are radio-poor and deviate significantly from the linear relation.

At millimeter wavelengths, the majority of the flare emission is accompanied by thermal bremsstrahlung of the hot flare plasma. Characteristics are low circular polarization and correlation with thermal soft X-rays.

4.1.2.8.1.2 Peak fluxes and burst rates

Figure 5 summarizes peak flux reports by various authors. The maximum flux is produced by different burst types, depending on frequency. Gyrosynchrotron emission dominates at centimeter wavelengths, decimetric pulsations in the decimeter range, Type II and moving Type IV at meter and decameter wavelengths. Note that Type I noise storms have relatively low peak values, but are present far more frequently than the other burst types. The inclined *thin black* lines indicate the brightness temperature assuming a source size of the solar disk. It is a lower limit to the actual value.

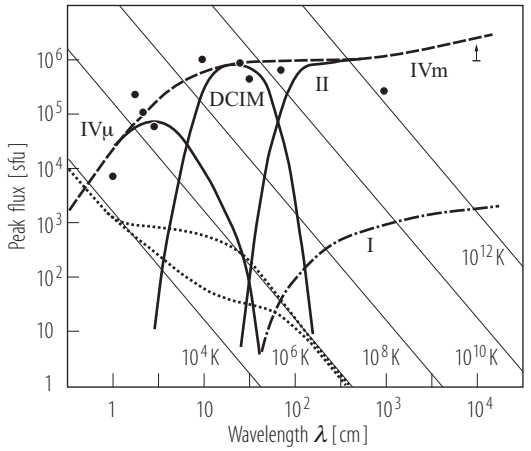

Fig. 5. Peak flux of flare radio emission vs wavelength (*dashed curve*). The reported data points given by *dots,* are collected from the literature [81Hac, 05Kan, 04Lan, 06Ben, 08Kai]. The maximum flux is caused by different types of flare radio bursts indicated by their usual abbreviation and *solid* curves. Noise storm limits are marked by "I" (*dash-dotted* curve). The quiet sun radio level is indicated by the *lower dotted curve*. During solar maximum, it adds up with the slowly varying component to the *upper dotted curve*. Thin lines indicate the brightness temperature assuming a source of the size of the solar disk. They give a lower limit of the burst brightness.

Moderate radio bursts are well above thresholds of everyday technical appliances. Large solar radio events constitute interference for terrestrial communication, navigation and radar. Figure 6 displays the peak burst flux distribution of large events. The data has been collected from observatory reports over the years. The long term average distribution is an approximate power-law of the form $(F_{\mathrm{peak}})^{-1}$. Cycle 20, a cycle with relatively low activity, had a lower rate. However, instrument effects, saturation and calibration errors cannot be excluded.

The number of bursts per day varies with the solar cycle (Fig. 7). The double peak in cycle number 22 from 1986–1995 is more pronounced than in sunspot number. During a large solar maximum, there is a burst larger than 1000 sfu (1000 sfu = 10^{-19} W m^{-1} Hz^{-1}) every other day in the 1–10 GHz range on average.

4.1.2.8.1.3 Source size and angular scattering

The sources of solar radio bursts can generally be resolved with current interferometers. Their typical size increases with wavelength. Type II and IV bursts at meter waves often have irregular shape and sometimes exceed the size of the visual solar disk. Type I and III bursts are simpler and smaller. Table 5 lists the average size for different burst types and frequencies.

High resolution interferometric observations show a lack of structure at small scale. The effect is generally believed to be caused by angular scattering in the corona near the source. Figures 8 and 9 show theoretical calculations fitted to observations of minimum source size. A strong increase in angular broadening with wavelength is evident (Fig. 8). The angular broadening corresponds to the minimum observable sources size and is the apparent size of a point source. It increases with distance from disk center (Fig. 9), as the ray path in the corona increases.

Scattering limits the observed brightness temperature of bursts. It is a tool to study the turbulence level in the low corona.

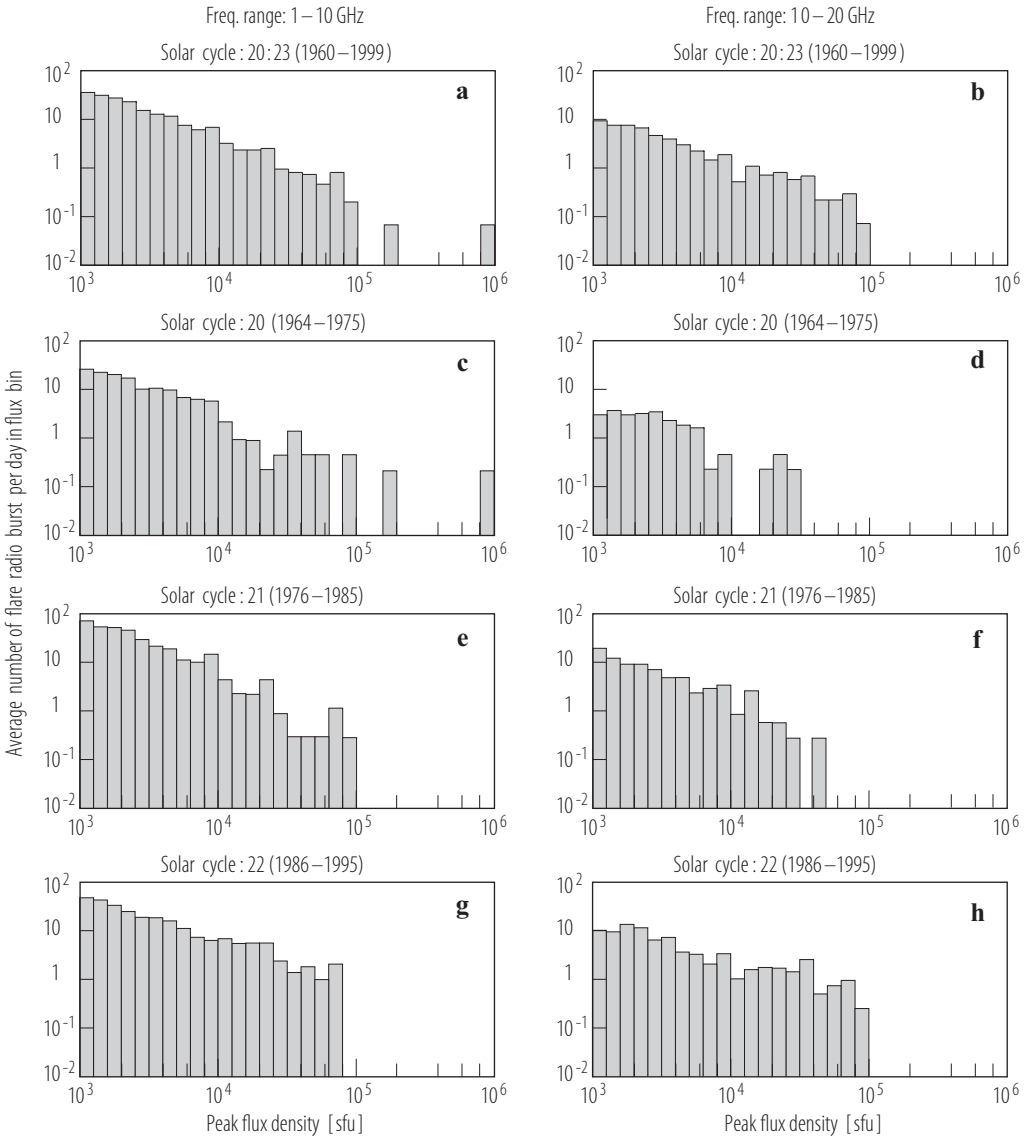

Fig. 6. Average number of flare radio bursts per day vs peak flux density. The left column shows the distribution for the frequency range 1–10 GHz (excluding 10 GHz). The right column shows the same for 10–20 GHz. The top row presents the average, the next three rows show individual solar cycles. Units: sfu = 10^{-22} W s^{-1} Hz^{-1}. The burst rate is multiplied by a factor of 1000 [04Lan].

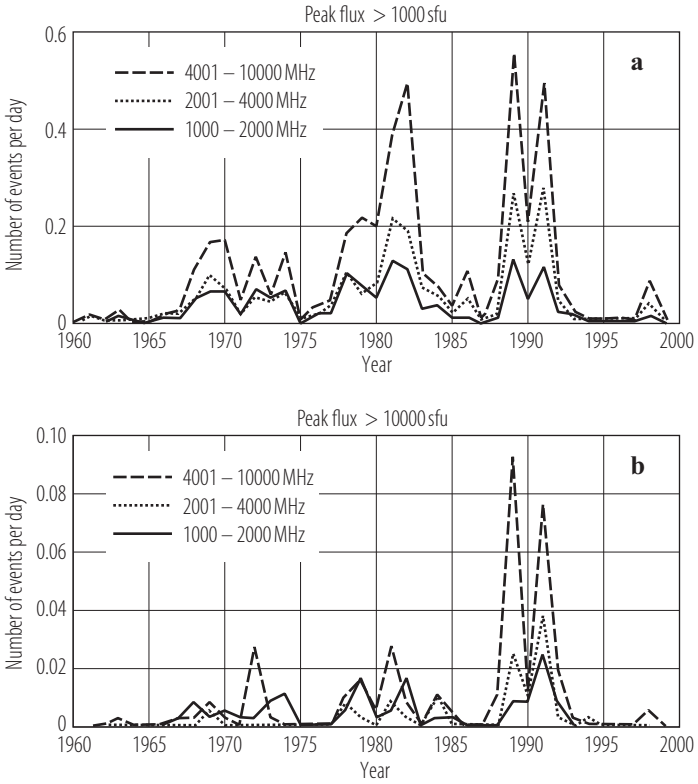

Fig. 7. Average number of flare radio bursts per day. The rate is given for three frequency ranges: *solid* line: 1000–2000 MHz, *dotted* line: 2001–4000 MHz, and *dashed* line: 4001–10000 MHz. *a*: peak flux > 1000 sfu, *b*: peak flux > 10000 sfu [04Lan].

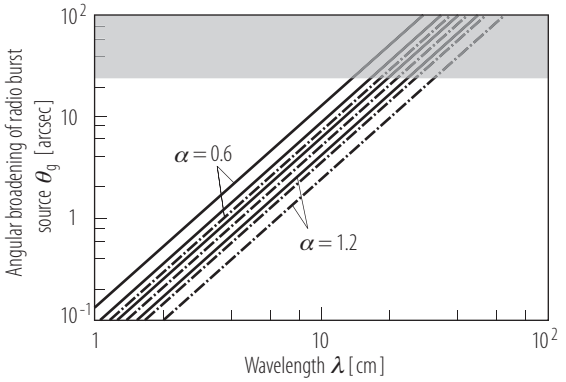

Fig. 8. Angular broadening of radio burst source versus wavelength by density fluctuations derived from scattering theory. The spectral distribution is assumed to be a power-law with an exponent of $\alpha + 2$. The scattering measure has been normalized using a wave structure function $D_{20}(10\text{km}) = 4$ rad^2 (*dashed-dotted line*) and 12 rad^2 (*solid line*). The grey-shaded area on the top indicates the region of lower accuracy of the analysis [94Bas].

Table 5. Average source size radio bursts of the active sun. The full width at half power is presented for emission at disk center (where given).

Burst type	Frequency	Size	Reference	Comment
Type III	60 kHz	37°	[07The]	includes also II
	115 kHz	25°	[07The]	includes also II
	540 kHz	15°	[98Rei]	
	38.5 MHz	12.5'–22.5'	[90The]	
	43 MHz	20'	[85Suz]	
	57.5MHz	10.5'–16.5'	[90The]	
	73.8MHz	5.5'–10.5'	[90The]	
	80 MHz	11'	[85Suz]	
	169 MHz	5'	[85Suz]	
	1.4 GHz	1.5'–2.2'	[90Wil]	unclassified
	5.7 GHz	10"	[05Mes]	unclassified
Noise storm	164 MHz	3.7'	[96Mal]	Continuum
	236 MHz	2.5'	[96Mal]	Burst sources
	327 MHz	2.5'	[96Mal]	are smaller
Centimetric	5 GHz	9"–10"	[85Sch]	
	17 GHz	5.3"	[04Kun]	
	90 GHz	< 5"	[91Kun]	

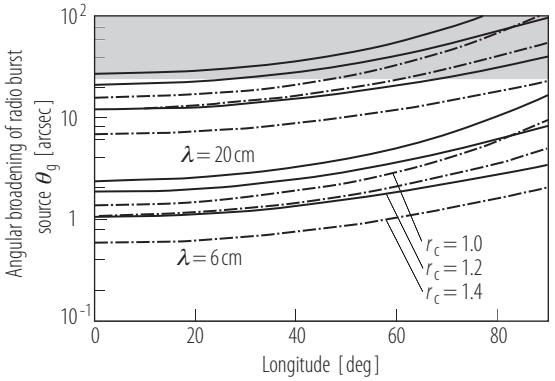

Fig. 9. Angular broadening versus distance from disk center calculated for two wavelengths. Different values for the inner cutoff r_c are indicated, below which the level of turbulence is assumed to be constant. The spectral power-law of the density fluctuations is assumed to have an exponent of $\alpha + 2 = 3$. The solid and dashed-dotted lines and the grey-shaded area are as in Fig. 8 [94Bas].

4.1.2.8.2 References for 4.1.2.8

General references

a Kundu, M.R.: *Solar Radio Astronomy* (1971), Interscience Publishers: New York.

b Krüger, A.: *Introduction to Solar Radio Astronomy and Radio Physics* 2nd ed. (1979), D. Reidel: Dordrecht.

c McLean, D.J., Labrum, N.R., eds.: *Solar Radiophysics*, Cambridge: Cambridge University Press (1985).

d Benz, A.O.: *Plasma Astrophysics – Kinetic Processes in Solar and Stellar Coronae*, 2nd ed. (2002), Kluwer Academic Publishers: Dordrecht.

Special references

66Han Hanasz, J.: Austral. J. Phys. **19** (1966) 635.

70Boi Boischot, A., de La Noe, J., Møller-Pedersen, B.: Astron. Astrophys. **4** (1970) 159.

73Alv Alvarez, H., Haddock, F.T.: Solar Phys. (1973) **30** 175.

77Elg Elgaroy, O.: *Solar Noise Storms* (1977), Pergamon Press: Oxford.

81Ben Benz, A.O., Wentzel, D.G.: Astron. Astrophys. **94** (1981) 100.

81Hac Hachenberg, O.: Landolt-Boernstein, New Series VI/2a (1981) 293.

85Sch Schmahl, E.J., Kundu, M.R., Dennis, B.R.: Astrophys. J. **299** (1985) 1017.

85Suz Suzuki, S., Dulk, G.A.: *Solar Radio Physics*, Cambridge: Cambridge University Press (1985) p. 291.

88Kos Kosugi, T., Dennis, B.R., Kai, K.: Astrophys. J. **324** (1988) 1118.

90Gue Guedel, M., Benz, A.O.: Astron. Astrophys. **231** (1990) 202.

90The Thejappa, G., Gopalswamy, N., Kundu, M.R.: Solar Phys. **127** (1990) 165.

90Wil Willson, R.F., Lang, K.R., Liggett, M.: Astrophys. J. **350** (1990) 856.

91Kun Kundu, M.R., White, S.M., McConnell, D.M.: Solar Phys. **134** (1991) 315.

92Ben Benz, A.O., Magun, A., Stehling, W., Su, H.: Solar Phys. **141** (1992) 335.

94Bas Bastian, T.S.: Astrophys. J. **426** (1994) 774.

94Isl Isliker, H., Benz, A.O.: Astron. Astrophys. Suppl. Ser. **104** (1994) 145.

96Mal Malik, R.K., Mercier, C.: Solar Phys. **165** (1996) 347.

98Bas Bastian, T.S., Benz, A.O., Gary, D.E.: Ann. Rev. Astron. Astrophys. **36** (1998) 131.

98Rei Reiner, M.J., Fainberg, J., Kaiser, M.L., Stone, R.G.: Journal of Geophysical Research **103** (1998) 1923.

00Kru Krucker, S., Benz, A.O.: Solar Phys. 191 (2000) 341.

04Lan Lanzerotti, L.J.: in: *Solar and Space Weather Radiophysics* (D.E. Gary and C.U. Keller, eds.), Kluwer Academ. Publ. (2004) p. 1.

04Kun Kundu, M.R., Nindos, A., Grechnev, V.V.: Astron. Astrophys. **420** (2004) 351.

05Kan Kane, S.R., McTiernan, J.M., Hurley, K.: Astron. Astrophys. **433** (2005) 1133.

05Mes Meshalkina, N.S., Altyntsev, A.T., Lesovoi, S.V., Zandanov, V.G.: Adv. Space Res. **35** (2005) 1785.

06Ben Benz, A.O., Perret, H., Saint-Hilaire, P., Zlobec, P.: Adv. Space Res. **38** (2006) 951.

07The Thejappa, G., MacDowall, R.J., Kaiser, M.L.: Astrophys. J. **671** (2007) 894.

08Kai Kaiser, M.L.: Private communication (2008).